

Analysis of the Impact of Rotating GNSS Antennae in Kinematic Terrestrial Applications

Jens-André PAFFENHOLZ, Tobias KERSTEN, Steffen SCHÖN and Hansjörg KUTTERER, Germany

Key words: GNSS, kinematic positioning, phase centre corrections, PCO, PCV, terrestrial laser scanning

SUMMARY

For direct geo-referencing of static terrestrial laser scans a method developed at the Geodetic Institute of the Leibniz Universitaet Hannover utilises an eccentrically mounted GNSS antenna on top of the laser scanner. The at least 360 degree rotation about its vertical axis is suitable for deriving the position as well as the azimuthal orientation of the sensor. In this approach the alternating antenna orientation with respect to an Earth-Centred, Earth-Fixed reference system will contribute to the error budget due to the right-hand circular polarisation of the satellite signals and the phase centre corrections (offsets and associated variations). For local precise applications the error magnitude has to be considered.

This paper focus on the assessment of systematic effects of an eccentrically rotating GNSS antenna. A simultaneous acquired tacheometer trajectory and a computed theoretic trajectory are used for verification. For the determination of the tacheometer trajectory a (360 degree) prism is directly attached below the GNSS antenna. The theoretic trajectory is computed based on the known geometry of the GNSS antenna mount on top of the laser scanner. A first data analysis with respect to systematic effects is carried out in the observation domain. A second data analysis is performed in the coordinate domain, which is of major interest because of the position and orientation estimation from coordinates. Hence, the analysis focuses on the impact of systematic errors in the coordinate domain. The results are evaluated with respect to their significance for the previously introduced application: the direct geo-referencing of static laser scans.

Analysis of the Impact of Rotating GNSS Antennae in Kinematic Terrestrial Applications

Jens-André PAFFENHOLZ, Tobias KERSTEN, Steffen SCHÖN and Hansjörg KUTTERER, Germany

1. INTRODUCTION

Today, several kinematic terrestrial applications make use of the Global Navigation Satellite System (GNSS) for absolute positioning as well as for heading determination of moving platforms. There is a great variety of applications in, e.g., machine guidance, precision agriculture, maritime ship guidance, positioning of mobile mapping vehicles as well as in the field of engineering geodesy. Usually, several GNSS antennae and additional navigation sensors are used to estimate the required transformation parameters from local sensor-defined coordinate systems to absolute or global coordinate systems, like an Earth-Centred, Earth-Fixed (ECEF) coordinate system. While guidance applications need real-time results, in most mobile mapping applications and engineering geodesy tasks a post-processing analysis is sufficient. Nevertheless, to obtain precise results for position and heading one has to keep a close eye on the error budget of the enlisted sensors. Due to the variety of applications, we will focus on a special one in engineering geodesy treating the estimation of the transformation parameters (position and heading) of a terrestrial laser scanner by means of kinematic GNSS measurements.

The main characteristic of the terrestrial laser scanning (TLS) technique for engineering geodesy is the immediate data acquisition in 3D space. This is realised with a high spatial resolution (a few millimetre for mean distances of approx. 25 m) as well as with a very high frequency (up to 50 profiles per second) in a relative or local sensor-defined coordinate system, respectively. The TLS technique can be used in a static and a kinematic mode. Static scanning is characterised by one single fixed translation and orientation of the laser scanner in relation to an absolute or global coordinate system. For kinematic scanning, where the data acquisition is commonly reduced to 2D profiles, the translations and orientations are time-dependent. Hence, the transformation parameters for each profile are different in relation to each other as well as to an absolute or global coordinate system. Whenever a combination of several static scans from different stations into one coordinate system (registration) is required, the transformation parameters for each scan have to be determined. For an additional link to an absolute or global coordinate system (geo-referencing), typically, control points in a known geodetic datum are necessary. By a direct observation of the required transformation parameters by means of GNSS equipment and arbitrary navigation sensors one can solve the registration and geo-referencing in one single step without the need of additional control points; for further details please refer to Paffenholtz et al. (2010).

For direct geo-referencing of static terrestrial laser scans a method (developed at the Geodetic Institute of the Leibniz Universitaet Hannover (LUH)) utilises an eccentrically mounted GNSS antenna on top of the laser scanner. The horizontal rotation of the laser scanner of at

least 360 degrees is suitable to derive the position as well as the azimuthal orientation of the sensor. In this approach the alternating antenna orientation with respect to an ECEF coordinate system will contribute to the error budget due to the right-hand circular polarisation of the satellite signals and the azimuthally varying phase centre corrections (PCC). In addition, near-field effects caused by the antenna adaption (made from aluminium) on the laser scanner, or possibly multipath from the vicinity may contribute to the error budget.

This paper is organised as follows: Section 2 gives a short overview about the error budget of GNSS measurements as well as antennae-related errors with the focus on the briefly introduced kinematic terrestrial application. Section 3 describes the performed experimental studies. The analysis and interpretation of the results are given in Section 4. Finally, Section 5 summarises the results and discusses possible future work.

2. ERROR BUDGET OF GNSS MEASUREMENTS

Uncertainties in GNSS measurements are a very complex interaction of satellite specific, propagation specific and station specific error sources. For short baselines (around 14 m), that are only considered in this paper, all propagation specific effects cancel out if single or double differencing is applied. To deal with satellite specific errors, products from processing centres, like e.g., the International GNSS Service (IGS) and for combined GPS and GLONASS precise ephemerides from the European Space Agency (ESA) European Space Operations Centre (ESOC) are used. Station dependent effects remain, such as multipath, or antenna phase centre corrections. These effects have to be considered by the user with appropriate correction models.

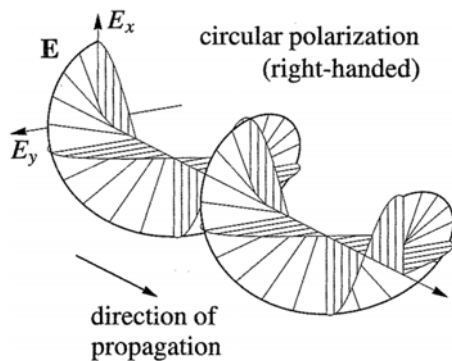


Figure 1: Polarisation of a satellite signal. The electric field vector $\mathbf{E} = [E_x \ E_y]$ varies with the ratio of perpendicular disposed electric field \mathbf{E} and the magnetic field \mathbf{B} (cf. Hofmann-Wellenhof 2008).

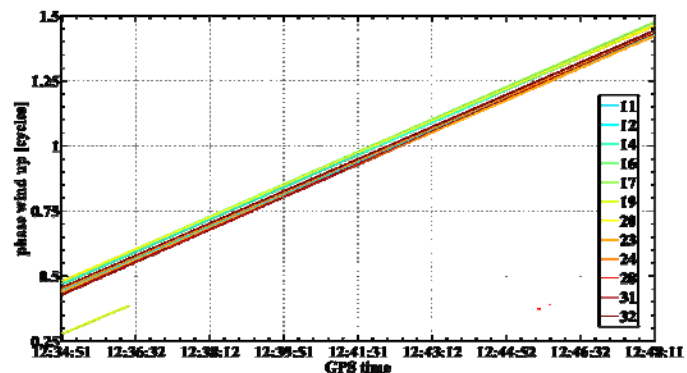


Figure 2: PWU-effect of an azimuthally rotating GNSS antenna for a typical time span of 13^{min} 20^{sec}). By calculating single-differences on a short baseline this remaining effect is identical for all satellites and thus absorbed into the receiver clock error.

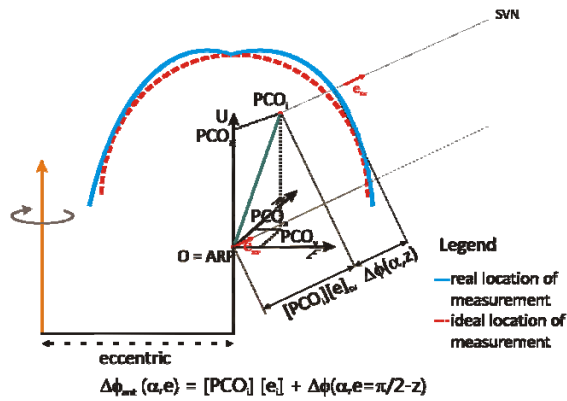


Figure 3: Sketch of PCC (PCO and associated PCV) for an eccentrically (and horizontally) rotating antenna.

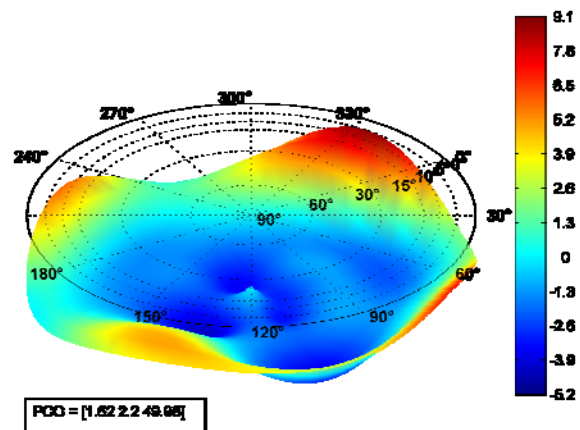


Figure 4: Stereographic plot of the absolute GPS L1 PCC for the antenna *Javad GrAnt G3T*, obtained with the Hannover concept at the Institut für Erdmessung (cf. Böder et al., 2001).

2.1 Polarisation of satellite signals

While GNSS signals are right-hand circular polarised (RHCP) electro-magnetic waves (cf. Figure 1) the relative orientation of receiver and satellite antennae has to be taken into account, as described in, e.g., Wu et al. (1993). In Figure 2 the cumulation of the phase wind up effect (PWU) when the antenna is horizontally rotated about its vertical axis is depicted. The PWU effect can reach up to one full cycle due to the signal polarisation. The contribution of an antenna horizontally rotating with constant velocity to the PWU effect is linear in time and identical for all satellites visible in the topo-centre. Computing single-differences on a short baseline, the net effect is constant for all satellites and thus it is absorbed by the receiver clock error, cf. Section 4.

2.2 Phase centre corrections

The actual phase measurements are related to the electrical phase centre of the receiver antenna while within the adjustment measurements are modelled with respect to the geometrically well defined antenna reference point (ARP). This difference is described by the phase centre corrections (PCC), a consistent set of phase centre offset (PCO) as well as their associated elevation and azimuth depending phase centre variations (PCV) for each frequency and GNSS system, cf. Figure 3. An example plot of absolute PCC is shown in Figure 4.

2.3 Reduction of systematic effects

For the adequate reduction and modelling of systematic effects, following approaches are suitable (see, e.g., Hofmann-Wellenhof 2008): (1) Compute linear combinations and differences of observations to eliminate systematic effects. (2) Apply deterministic correction models. (3) Estimate additional parameters in adjustment process. Therefore, it is necessary to

analyse the separability of parameters. (4) Error modelling by stochastic processes. Here, the characterisation of the behaviour of errors types is necessary.

In this study we work with the Wa1 software (Wanninger, 2009a) using single-differences between receivers to eliminate orbit errors, satellite clock errors as well as errors due to propagation delays in the atmosphere. The small baseline of about 14 m used in the experiments eliminates all atmospheric effects.

3. EXPERIMENTAL STUDIES

This section describes the performed experimental studies to analyse the impact of rotating GNSS antennae in the previously introduced kinematic terrestrial application. The equipment used for the experimental studies is characterised, with a special focus on the GNSS component. All other used sensors are briefly introduced.

3.1 Used equipment and location for the experimental studies

The experimental studies were performed at the roof of the building of the Geodetic Institute (Messdach), LUH. On this roof a geodetic network with 9 pillars is located (cf. Figure 5). In all experiments pillar 8 is used as reference. The reference station is equipped with a *Leica AR25* (LEIAR25.R2) antenna connected to a *Javad TRE G3T Delta* receiver operating with a data rate of 10 Hz. The antenna under test, located on pillar 6 is a *Javad GrAnt G3T* connected to a *Javad TRE G3T Delta* receiver operating with a data rate of 20 Hz. The relative baseline between both pillars is approx. 14 m.

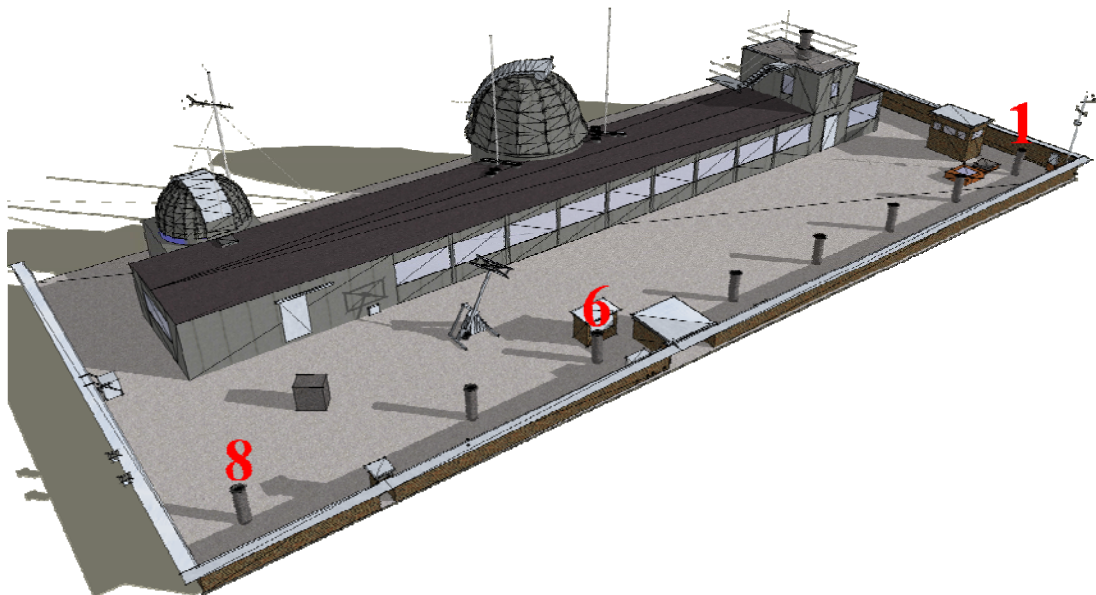


Figure 5: Sketch of the roof of the building of the Geodetic Institute (Messdach), LUH (Zaddach, 2010); numbered pillars were used for the experimental studies.

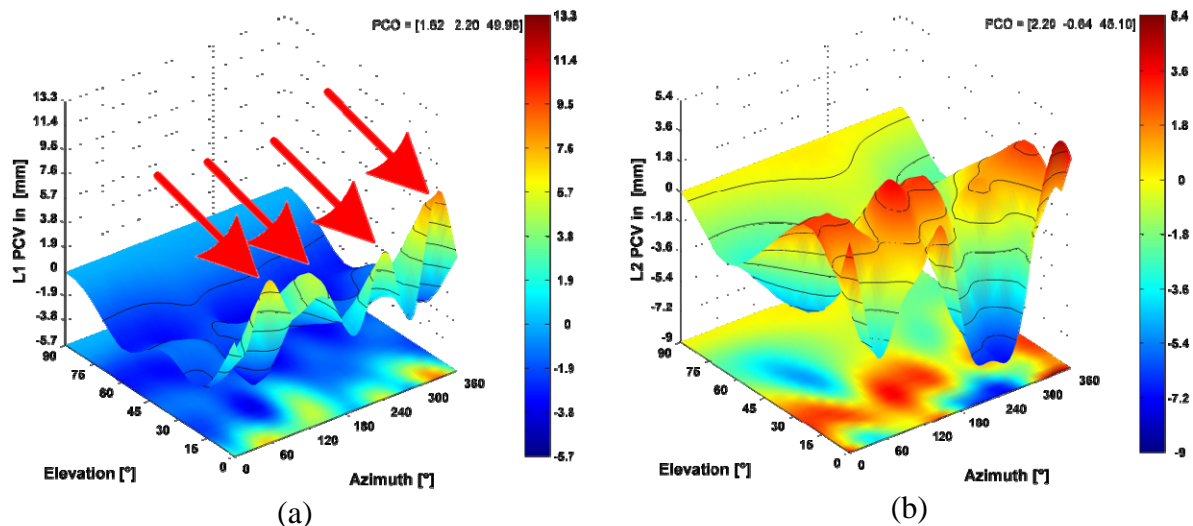


Figure 6: Individual PCC of GPS L1 (a) and GPS L2 (b) for the antenna *Javad GrAnt G3T*.

Both GNSS antennae are individually and absolutely calibrated based on the Hannover concept at the Institut für Erdmessung (IfE), LUH. In Figure 6 the PCV pattern for the GPS frequency L1 and L2 for the *Javad GrAnt G3T* antenna are depicted. The 3D rectangular plots clearly show the dependency of the PCV pattern on elevation and azimuth. Four sharp maxima can be recognized (cf. arrows in Figure 6 (a)), which are caused by the geometry of the antenna element itself and also by the geometrical dimension of the antenna housing. The L1 PCV corrections (cf. Figure 6 (a)) have a magnitude of 2-4 mm for mean elevation angles greater than 45° and rise to 6 mm for elevation angles below 45° . On L2 (cf. Figure 6 (b)) a similar behaviour can be identified. The maximum differences in elevation dependent PCV are 9 mm. The PCO up component is 49.98 mm for L1 and 45.10 mm for L2, respectively, up to 5 times greater than the pattern.

In Section 1 we introduced a method for a direct geo-referencing of static terrestrial laser scans which explicitly utilises the rotation of an eccentrically mounted GNSS antenna on top of a laser scanner to derive the position and orientation parameters. Therefore, these GNSS measurements should be analysed in detail with respect to the error budget discussed in Section 2. For a real scenario the laser scanner Zoller+Fröhlich Imager 5006 is used within the experiment (cf. Figure 8 (a)). Additionally, a 360 degree prism is directly attached below the ARP of the GNSS antenna to acquire an experimental trajectory (cf. Figure 8 (c)) with a *Leica TS30* tacheometer (cf. Figure 8 (b)). This tacheometer tracks with a data rate of 2 Hz and is located on pillar 1 (cf. Figure 5) with an approx. distance of 27 m to pillar 6. Besides, a theoretic trajectory is computed based on the known geometry of the GNSS antenna mount on top of the laser scanner. Both trajectories are used as reference trajectories for the further investigations. They independently describe the circular motion of the laser scanner.

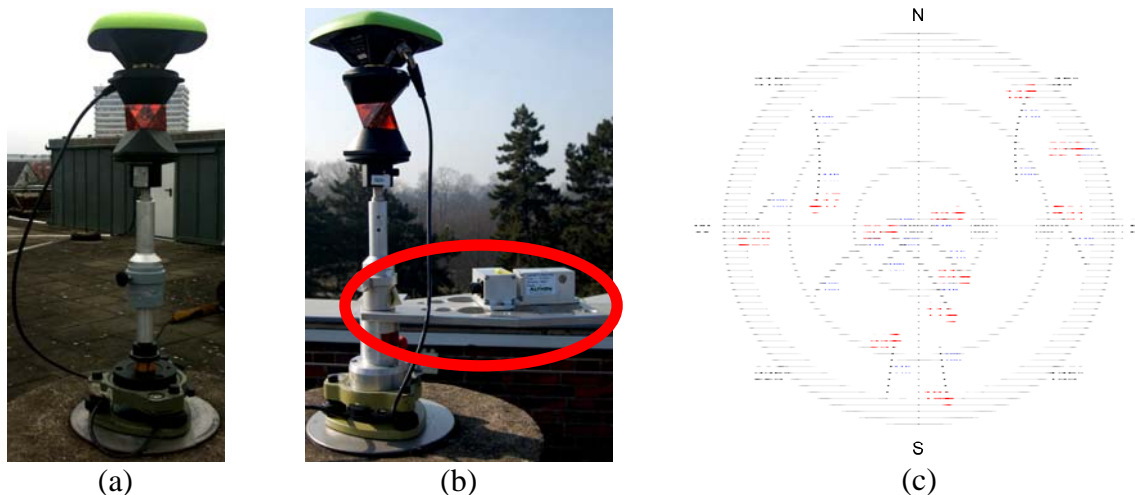


Figure 7: Setup of DOY049: antenna with standard tripod on pillar 6 (a) and setup of DOY041 with wing adaption of laser scanner (b). Sky plot of GPS satellites on pillar 6 for DOY049 09:50:38 - 11:25:38 GPS time (c). The PRN number marks the elevation at start of measurement, the arrows are related to the flight direction.

3.2 Pre-investigations - measurements with a non-rotating antenna (DOY049 and 041)

We gave special attention to assess the performance of the used GNSS antenna for estimating coordinates with a non-rotating antenna. Within these measurements two different setups were used at pillar 6. The combination of antenna and direct attached 360 degree prism as well as the height above the pillar 6 (cf. Figure 7 (a) and (b)) are identically for both scenarios. The difference is the additional use of the wing adaption for the antenna on top of the laser scanner in the measurements on DOY041 (cf. marker in Figure 7 (b)). The observation time is for DOY049 09:50:38 - 11:25:38 GPS time and for DOY041 10:22:06 - 11:57:06 GPS time, respectively. The sky plot in Figure 7 (c) depicts the GPS constellation of DOY049 with four satellites with high elevations (above 30°) and a good signal to noise ratio in a range from 45 to 53 dBHz. Additionally, six other GPS satellites have an elevation above 10° . Furthermore, there are five GLONASS satellites visible for the whole observation time. The time difference of DOY041 and DOY049 corresponds to the difference between sidereal and solar day length over eight days. By this observation timing the same satellite constellation for GPS and GLONASS as well as nearly identical repeat tracks for the satellite vehicles are assumed. Hence, it is possible to get a rough idea about the influence of the wing adaption on the GNSS measurements.

3.3 Kinematic measurements with an eccentrically rotating antenna (DOY025)

To analyse the impact of rotating GNSS antennae in kinematic terrestrial applications measurements with a laser scanner rotating about its vertical axis were performed on DOY25. The observation time is on DOY025 11:27:34 - 12:48:41 GPS time. The time difference of these measurements corresponds again to the difference between sidereal and solar day length over 16 and 24 days, respectively. This allows the comparison of all static and kinematic

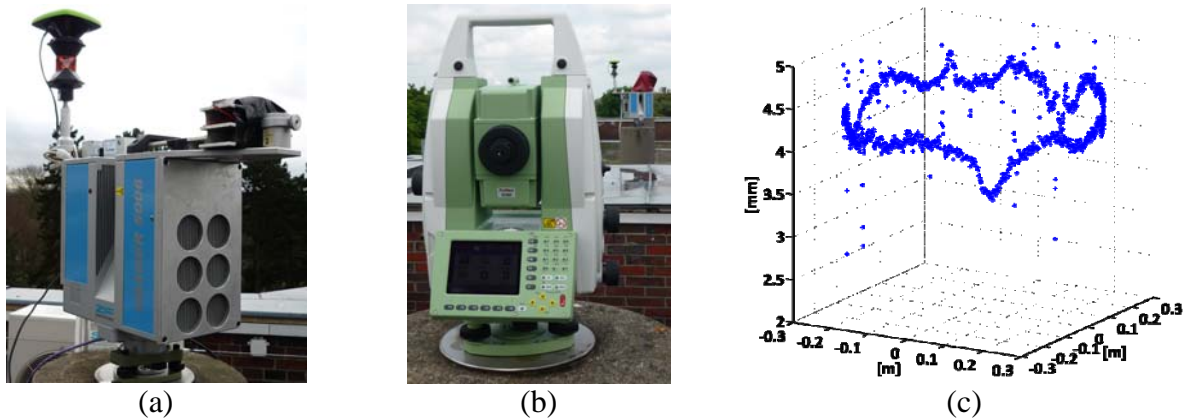


Figure 8: Laser scanner with adapted GNSS antenna and 360 degree prism on pillar 6 (a), Leica tacheometer TS30 for tracking the circular motion of the laser scanner on pillar 1 (b), and sample trajectory in local geodetic coordinates of the tracked 360 degree prism (c).

measurements within the experimental studies. During the above given time span several independent recurring runs were undertaken (each with approx. 15 min duration).

Figure 8(a) illustrates the GNSS antenna with directly attached 360 degree prism eccentrically adapted on top of the laser scanner. To compensate the weight of the GNSS antenna and prism similar weights were placed on the opposite wing. Furthermore, the laser scanner was oriented to the direction of gravity. Remaining spatial residuals can be observed by two adapted single-axis inclinometer. All observations (GNSS, tacheometer, optional inclinometer) within the kinematic measurements are synchronised by a real-time computer (Paffenholz et al., 2010).

4. ANALYSIS AND INTERPRETATION OF THE RESULTS

4.1 Observation domain

To detect systematic effects we analysed the double-differences (DD) of phase measurements for DOY041 and DOY049, respectively. In Figure 9 the signal strength (CN/0) versus elevation of the satellite in antenna topo-centric system is plotted as well as the DD. For a satellite near zenith (cf. PRN 24 Figure 9 (a)) a very high CN/0 of 53 dBHz is expected. The received DD are in a range of ± 5 mm with small amplitude. In comparison to PRN 24 the PRN 17 has a low elevation (below 30°) with higher DD residuals (cf. Figure 9 (b)). This behaviour may be caused by the antenna itself. However, the residuals also show systematic variations with a magnitude of up to 1 cm. These variations decrease in case of rising elevations. To sum up the DD analysis for time series of DOY041 and DOY049 we can conclude that there is no significant influence due to the wing adaption.

To analyse the impact of the PCC as well as of the question if it is necessary to take a rotated PCC correction for this GNSS-TLS application into account, corrections in different combinations were applied to the measurements. For every epoch a new set of PCC for an

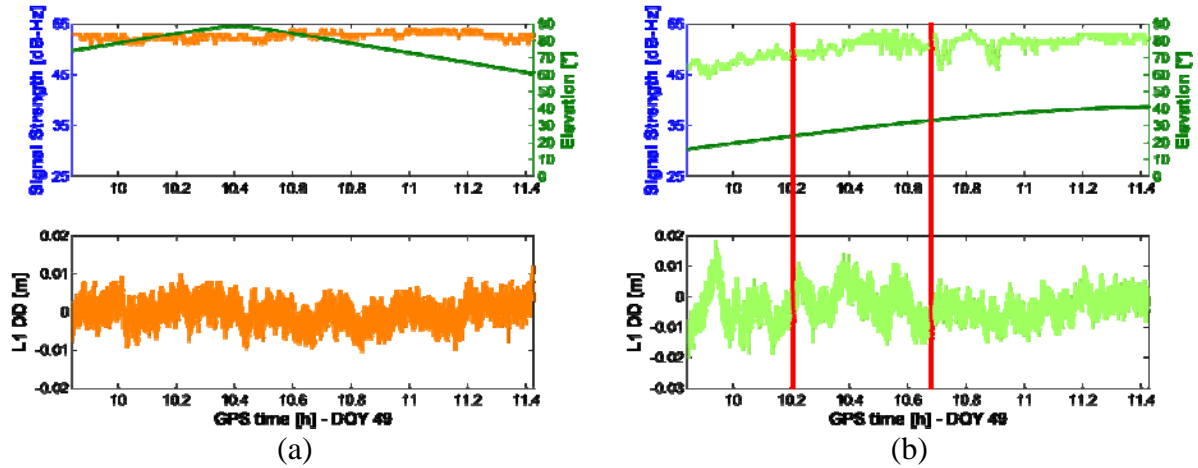


Figure 9: L1 DD and signal strength for PRN 24 (a) with visibility in zenith and L1 DD and signal strength for the ascending PRN 17 (b).

eccentrically rotated antenna is calculated and projected into the line of sight to individual satellites.

$$PCO_c = f(PCO, \alpha_0, r, \Delta\alpha) \quad (1)$$

$$PCV_c = f(PCV, \alpha_0, r, \Delta\alpha) \quad (2)$$

$$\Phi_{c_i}^j = \Phi_i^j - PWU_{c_i}^j + PCO_{c_i}^j - PCV_{c_i}^j \quad (3)$$

The corrected PCO_c (Equation 1) and PCV_c (Equation 2) are functions of the original PCO and PCV , the initial azimuth of antenna orientation α_0 (at the beginning of the scan), the radius r and $\Delta\alpha$, which denotes the angle increment between two rotation steps. In Equation 3 the index i denotes the individual frequency and j stands for the satellite number, respectively. In Figure 10 the original PCC were subtracted from the rotated PCC. For GPS L1, magnitudes of up to 5 mm occur at low elevations. This is expected, as declared in Section 3.1. Within the approx. 15 minutes, where the laser scanner performs one full circle, the satellite only moves a small amount. Consequently, the azimuthal variations of the PCV in a small elevation band dominate the differences shown in Figure 10.

4.2 Coordinate domain

This section discusses the results in the coordinate domain. First the results of the pre-investigate measurements with different environments are treated according to Figure 11. Figure 12 and Figure 13 show the results of the kinematic measurements for one specific run. For all GNSS analyses the *Wal* software is used.

As already stated in the previous section, we do not find any significant influence due to the different antenna environment on DOY041 and DOY049. By implication, this is the same in the coordinate domain. Figure 11 depicts the local geodetic coordinates (North-East-Up - NEU) of the performed measurements with the non-rotating antenna. Two different GNSS

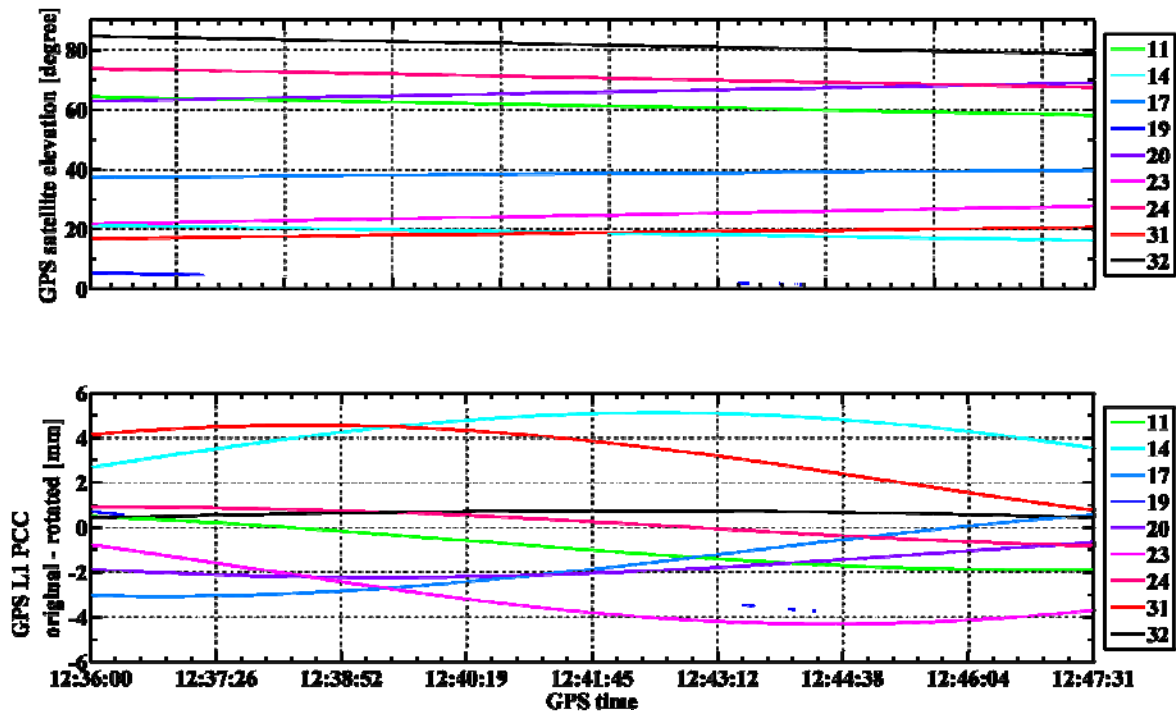


Figure 10: Top: Elevation of GPS satellites. Bottom: Original PCC minus rotated PCC for GPS L1 signals; DOY025, run15.

analysis are performed: A static estimation of the coordinate (solid line for DOY041 and dotted line for DOY049) and a kinematic estimation of the coordinates (circles for DOY041 and stars for DOY049). We can assess the kinematic coordinate estimation potential of the used GNSS antenna within a maximum range of 1 cm for the north and east component and up to 2 cm for the up component (cf. Figure 11).

For the investigation of the kinematic measurements with the eccentrically rotating antenna two GNSS trajectories are estimated. The difference between these two estimations is the set of applied PCC. One estimation is done with the original PCC, a non-rotating antenna is assumed. The other one is performed with the modified observations by rotating the PCC as explained in the previous section. Hereby, the GNSS range observations are modified using WaRINEX (Wanninger, 2009b). The rotated PCC were applied within the RINEX observation files. Afterwards, a re-processing of the modified GNSS observations is done. To indicate the influence of the rotated PCC in the coordinate domain these two trajectories are compared on basis of their NEU coordinates in Figure 12. The displayed time series are results of the difference of the GNSS trajectory and the corresponding experimental tacheometer trajectory. Figure 13 depicts the difference between the two GNSS trajectories with the different PCC applied to GPS frequencies. One can see a magnitude from 0 mm to -4 mm for the north component and the other way round for the east component. As expected, the up component is not affected by any rotation and we see a range of discrepancy of 0.4 mm.

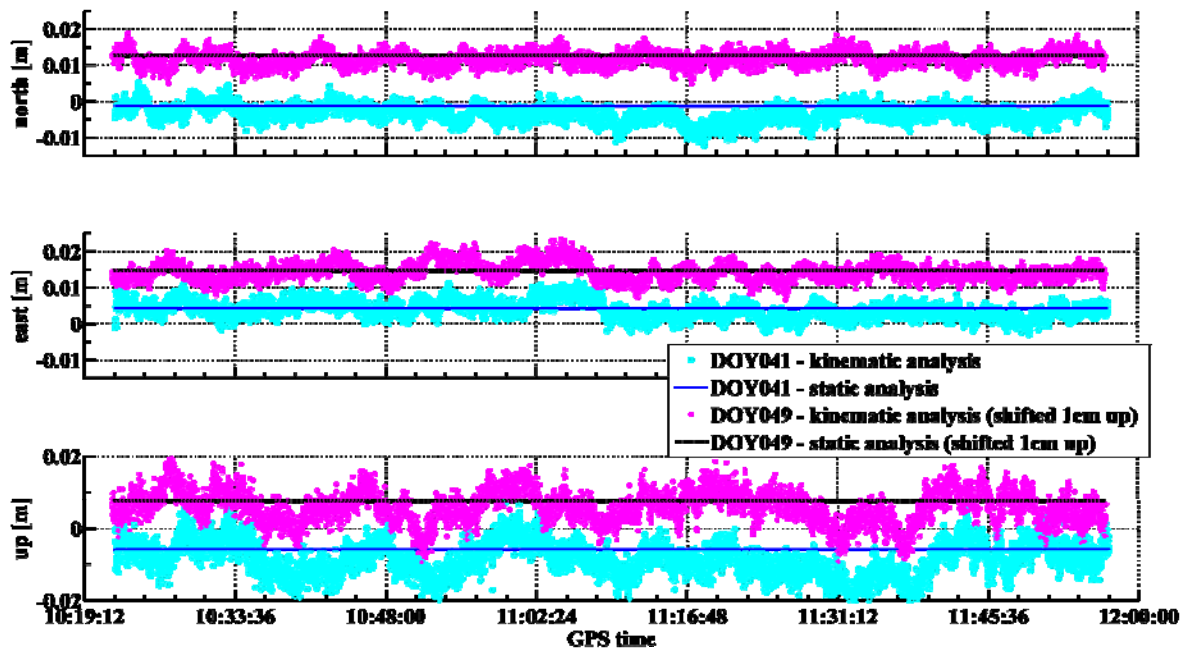


Figure 11: NEU coordinate differences of non-rotating antenna with respect to well known ITRF05 coordinate of pillar 6 (1 Hz data rate and 10° cut-off angle) in different scenarios: DOY041 with wing adaption: kinematic (circles) and static (solid line) analysis; DOY049 with standard tripod: kinematic (stars) and static (dotted line) analysis (times series of DOY049 are shifted 1 cm up for visualisation purposes).

4.3 Different mathematical approaches within the GNSS analysis

This sections deals with the GNSS analysis in the previously introduced direct georeferencing task. First some general remarks on the GNSS analysis are given. Afterwards two different mathematical approaches within the GNSS analysis are discussed.

In general, the kinematic GNSS analysis strategy depends on the number of used GNSS equipments on top of the laser scanner. Each ARP (of the eccentrically mounted antenna) is subject to a circular motion due to the rotation of the laser scanner (around its vertical axis). Currently, only one GNSS equipment is used on top of the laser scanner. If two GNSS equipments were used, the GNSS analysis can be done in two different ways. One way is the calculation of one single baseline for each equipment. The combination of the two ARP trajectories has then to be realised in a subsequent filter algorithm in state space. The other way requires the calculation of a relative baseline between the two GNSS antennae installed on top of the laser scanner. This is comparable to the GNSS compass approach, e.g., given in Teunissen et al. (2011). Within the filter algorithm there is no combination step necessary. Apart from the 3D positions of the ARP trajectory, the corresponding variance-covariance matrices are used within the filter algorithm to derive the position and, especially, the azimuthal orientation.

For the kinematic GNSS data processing, several approaches are possible. The common characteristic of all approaches is the data post-processing. In addition, a GNSS reference

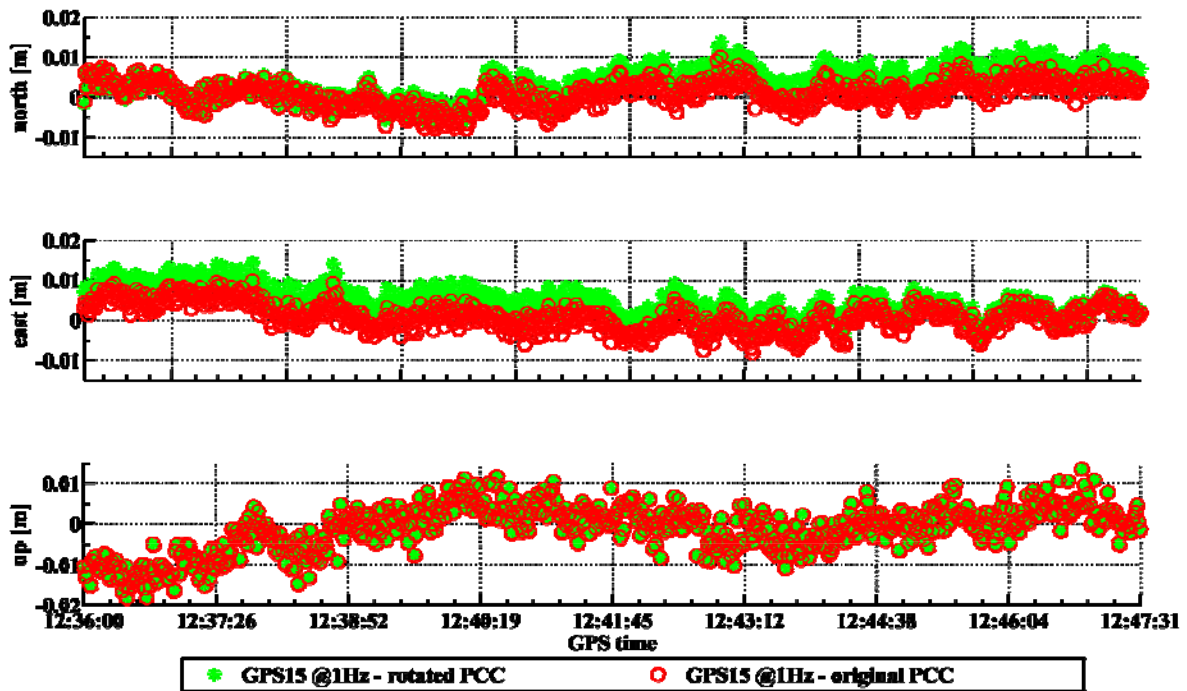


Figure 12: NEU coordinates for computed differences between experimental reference trajectory and rotated PCC pattern (stars) as well as original PCC pattern (circles).

station is required to obtain precise 3D positions for the circular motion of the ARP, as well as for an additional transformation to a global coordinate system. Real-time processing would be possible. But however, the potential to determine reliable transformation parameters with the real-time derived 3D positions has to be investigated in future.

The 3D positions and their variances are of great importance in deriving the quality of the position and orientation information of the laser scanner. Two points have to be taken into account: On the one hand, the error budget of the GNSS component has to be considered which was already discussed in the preceding sections. On the other hand, the mathematical approach within the GNSS analysis itself affects the quality of the 3D positions and the derived position and orientation parameters.

Different mathematical approaches within the GNSS analysis are (1) epoch-wise, independent solutions and (2) use of filter algorithms, e.g., Kalman filtering, within the GNSS analysis with a-priori known motion models. To get a rough idea about the different results two software products were used. The Wa1 software which provides an independent solution for each epoch, and the application GNSMART (Wübbena et al., 2001) which estimates the coordinates within a Kalman filter. In Figure 14 the results of one specific run of the kinematic measurements are depicted. They show a quite good result for the correspondence of the filter-based solution and the experimental trajectory (circles). The differences between the epoch-wise solution and the experimental trajectory (stars) are slightly larger and more noisy. The direct comparison of the epoch-wise and the filter-based solution fit in a range of 5 mm, here the noise level of the epoch-wise solution dominates.

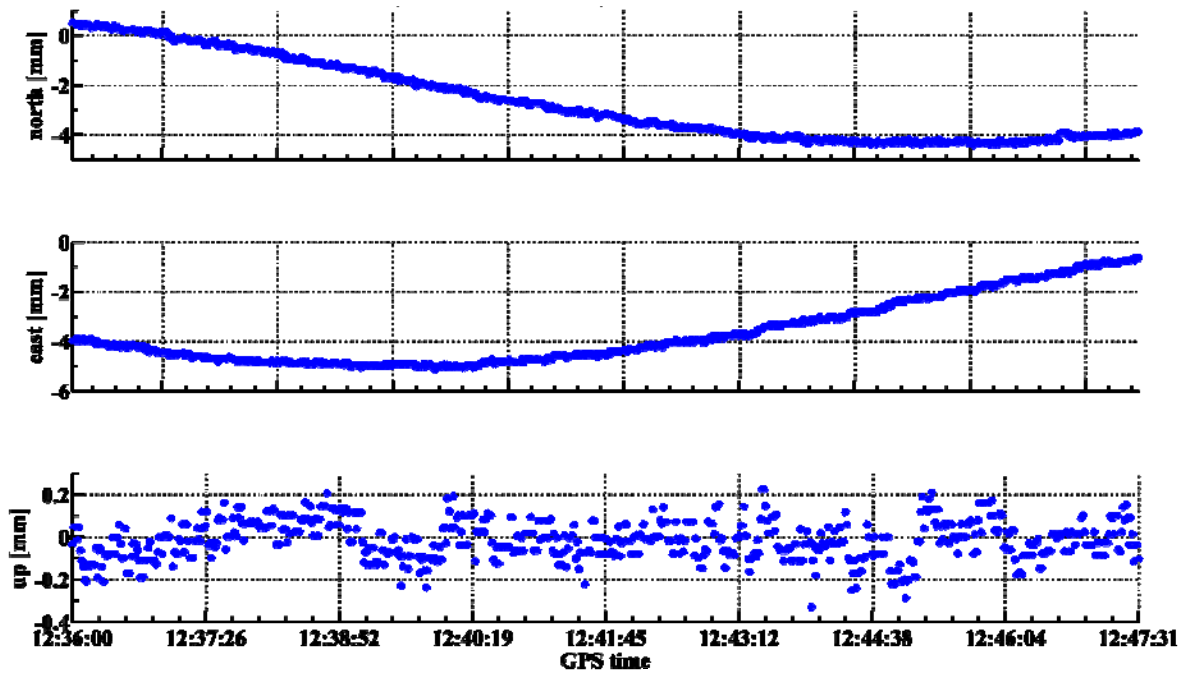


Figure 13: Difference between GNSS trajectories (here GPS only solution) with original PCC and rotated PCC applied to GPS frequencies L1 and L2.

5. CONCLUSIONS AND OUTLOOK

This paper discusses the analysis of the impact of rotating GNSS antennae in kinematic terrestrial applications. It is focused on a special terrestrial application, the direct georeferencing (estimation of transformation parameters from local to global coordinate systems) of terrestrial laser scans by means of GNSS equipment. Therefore, systematic errors due to a horizontal rotation of a GNSS antenna of about 360 degree are studied.

An DD analysis in the observation domain shows no significant impact of the used wing adaption in the direct vicinity. The PWU effect is constant and, therefore, treated like receiver clock offset in the adjustment. As expected, the rotated PCC against the original PCC has an effect of up to 5 mm in the observation domain which corresponds to the horizontal offset components. The analysis in the coordinate domain also indicates an effect of up to 5 mm. Although, the analysis shows that the PCC effect is dominated by the PCO components. Comparing the two different GNSS analysis strategies (epoch-wise and filter-based), the filter-based solution shows, as expected, a slightly better result. In addition, we can conclude that within a epoch-wise GNSS analysis the effect of rotated PCC has no significant impact on the transformation parameters in the geo-referencing procedure. Any significant improvement for the transformation parameter estimation in case of using a filter-based approach has to be investigated in future work.

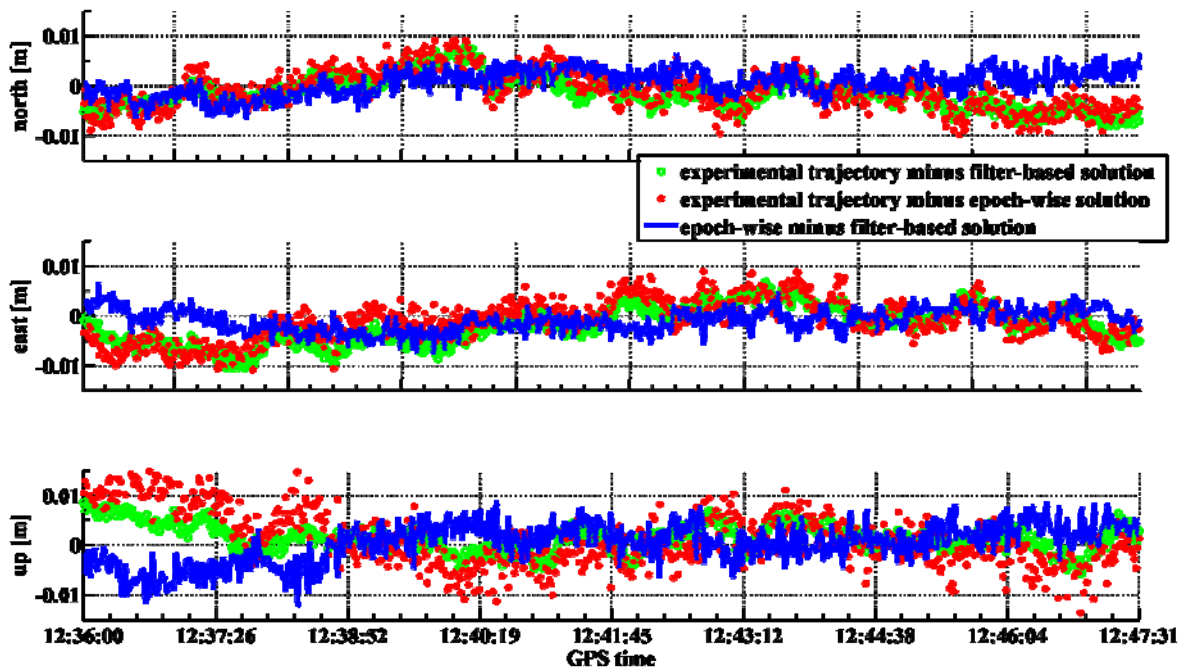


Figure 14: Difference of NEU coordinates of epoch-wise solution (Wa1) and filter-based solution (GNSMART). Differences between experimental trajectory and filter-based solution (circles) as well as epoch-wise solution (stars).

ACKNOWLEDGMENTS

Our special thanks go to Nico Lindenthal for the support with the kinematic GNSS analysis with GNSMART.

REFERENCES

- Böder, V.; Menge, F.; Seeber, G.; Wübbena G.; Schmitz, M. (2001): *How to Deal With Station Dependent Errors – New Developments of the Absolute Field Calibration of PCV and Phase-Multipath With a Precise Robot*. In: Proceedings of the 14th International Technical Meeting of the Satellite Division of the Institute of Navigation, ION GPS-2001, Salt Lake City, Utah, September 11-14.
- Hofmann-Wellenhof, B.; Lichtenegger, H. Wasle, E. (2008): *GNSS Global Navigation Satellite Systems GPS, GLONASS Galileo & more*. Springer Wien, New York.
- Paffenhof, J.-A., Alkhatib, H.; Kutterer, H. (2010): Direct geo-referencing of a static terrestrial laser scanner. *Journal of Applied Geodesy* 4 (3), pp. 115-126.
- Teunissen, P. J. G.; Giorgi, G.; Buist, P. J. (2011): *Testing of a new single-frequency GNSS carrier phase attitude determination method: land, ship and aircraft experiments*. *GPS Solutions* 15 (1), pp. 15–28.
- Wanninger, L. (2009): *GNSS baseline processing program Wa1*, www.wasoft.de/wa1/index.html, last access 16.03.2011
- Wanninger, L. (2009): *Editing of GNSS observations with WaRINEX*, www.wasoft.de/wrn/index.html, last access 16.03.2011.
- Wu, J.; Wu, S.; Hajj, G.; Bertiger, W.; Lichten, S. (1993): *Effects of antenna orientation on GPS carrier phase*. *Manuscripta geodetica* 18 (2), Springer New York, pp. 91-98.
- Wübbena, G.; Bagge, A.; Schmitz, A. (2001): *RTK Networks based on Geo++[®] GNSMART - Concepts, Implementation, Results*. In: Proceedings of the 14th International Technical Meeting of the Satellite Division of the Institute of Navigation. ION GPS-2001, Salt Lake City, Utah, September 11-14.
- Zaddach, S. (2010): *Laserscans und georeferenziertes 3D-Umgebungsmodell*. Teilprojekt Abschlussbericht. (unpublished).

BIOGRAPHICAL NOTES

Jens-André Paffenhof received his Dipl.-Ing. in Geodesy and Geoinformatics at the Leibniz Universität Hannover. Since 2006 he has been research assistant at the Geodetic Institute of the Leibniz Universität Hannover. His main research interests are: terrestrial laser scanning, industrial measurement systems, and process automation of measurement systems. He is active in the Working Group 4.2.3 “Application of Artificial Intelligence in Engineering Geodesy” of the IAG Commission 4 (Positioning and Applications).

Tobias Kesten received his Dipl.-Ing. in Geodesy and Geoinformatics at the University of Berlin in 2009. He is currently employed as research assistant at the Institut für Erdmessung of the Leibniz Universität Hannover. His main research interests are: absolute receiver

antenna calibration, receiver technology and GNSS software application development.

Prof. Dr. Steffen Schön received his Dipl.-Ing. and Ph.D. in Geodesy at the University of Karlsruhe in 1999 and 2003, respectively. Since 2006 he has been a Full Professor at the Institut für Erdmessung of the Leibniz Universität Hannover. His research areas are: high sensitivity GNSS, indoor positioning and navigation with IMU and MEMS sensors, software receiver as well as correction and assessment of systematic errors in GNSS processing like GNSS station monitoring, high precision external clocks in GNSS, and absolute antenna calibration.

Prof. Dr. Hansjörg Kutterer received his Dipl.-Ing. and Ph.D. in Geodesy at the University of Karlsruhe in 1990 and 1993, respectively. Since 2004 he has been a Full Professor at the Geodetic Institute of the Leibniz Universität Hannover. His research areas are: adjustment theory and error models, quality assessment, geodetic monitoring, terrestrial laser scanning, multi sensor systems, and automation of measurement processes. He is active in national and international scientific associations. In 2009 he became a Vice President of the DVW – Gesellschaft für Geodäsie, Geoinformatik und Landmanagement. In addition he is member of the editorial boards of three scientific journals.

CONTACTS

Jens-André Paffenholz
Email: paffenholz@gih.uni-hannover.de
Prof. Dr. Hansjörg Kutterer
Email: kutterer@gih.uni-hannover.de

Tobias Kersten
Email: kersten@ife.uni-hannover.de
Prof. Dr. Steffen Schön
Email: schoen@ife.uni-hannover.de

Geodätisches Institut
Leibniz Universität Hannover
Nienburger Str. 1, 30167 Hannover, Germany

Institut für Erdmessung
Leibniz Universität Hannover
Schneiderberg 50, 30167 Hannover, Germany